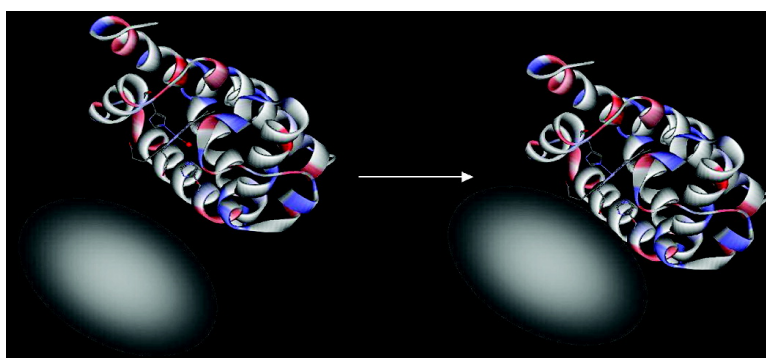


## Surface-Enhanced Resonance Raman Spectroscopic Characterization of the Protein Native Structure

Manliang Feng, and Hiroyasu Tachikawa

*J. Am. Chem. Soc.*, **2008**, 130 (23), 7443-7448 • DOI: 10.1021/ja8006337 • Publication Date (Web): 20 May 2008

Downloaded from <http://pubs.acs.org> on February 8, 2009



### More About This Article

Additional resources and features associated with this article are available within the HTML version:

- Supporting Information
- Access to high resolution figures
- Links to articles and content related to this article
- Copyright permission to reproduce figures and/or text from this article

[View the Full Text HTML](#)

## Surface-Enhanced Resonance Raman Spectroscopic Characterization of the Protein Native Structure

Manliang Feng and Hiroyasu Tachikawa\*

Department of Chemistry, Jackson State University, 1400 Lynch Street, P.O. Box 17910, Jackson, Mississippi 39217

Received January 25, 2008; E-mail: hiroyasu\_tachikawa@yahoo.com

**Abstract:** Surface-enhanced resonance Raman scattering (SERRS) spectra of biological species are often different from their resonance Raman (RR) spectra. A home-designed Raman flow system is used to determine the factors that contribute to the difference between the SERRS and RR of met-myoglobin (metMb). The results indicate that both the degree of protein–nanoparticles interaction and the laser irradiation contribute to the structural changes and are responsible for the observed differences between the SERRS and RR spectra of metMb. The prolonged adsorption of the protein molecules on the nanoparticle surface, which is the condition normally used for the conventional SERRS experiments, disturbs the heme pocket structure and facilitates the charge transfer process and the photoinduced transformation of proteins. The disruption of the heme pocket results in the loss of the distal water molecule, and the resulting SERRS spectrum of metMb shows a 5-coordinated high-spin heme. The flow system, when operated at a moderately high flow rate, can basically eliminate the factors that disturb the protein structure while maintaining a high enhancement factor. The SERRS spectrum obtained from a  $1 \times 10^{-7}$  M metMb solution using this flow system is basically identical to the RR spectrum of a  $5 \times 10^{-4}$  M metMb solution. Therefore, the Raman flow system reported here should be useful for characterizing the protein–nanoparticles interaction and the native structure of proteins using SERRS spectroscopy.

### Introduction

Raman spectroscopy is a powerful technique for studying biological molecules because it provides fingerprints of molecules and contains rich structural information. Resonance Raman (RR) spectroscopy has been used frequently for studying the active site structure of proteins because it uses laser excitation in the electronic absorption band of the prosthetic groups producing a large enhancement of Raman scatterings for vibrational modes of these groups. This is very important for the selective detection and the structural characterization of biological materials. The surface-enhanced Raman scattering (SERS) provides enormous enhancement to both the normal Raman and the resonance Raman signals<sup>1–3</sup> and has gained great interest in the study of biological molecules since its discovery over 30 years ago. Because of the large signal enhancements, the SERS spectroscopy is suitable for studying analytes of small quantities and very low concentrations. The recent advances in surface-enhanced Raman spectroscopy, which have benefited from the rapidly developing nanotechnology, have further enhanced the application of this technique in analytical, material, and biochemical researches. The greatly improved sensitivity of surface-enhanced resonance Raman scattering (SERRS) spectroscopy has made Raman spectroscopy, once an insensitive method, possible for single molecule surface-enhance Raman

scattering (SM-SERS).<sup>4–10</sup> However, the fact that the SERS spectra are normally different from the corresponding RR spectra has raised concerns about whether this technique is suited for studying the native structure of biological molecules. The difference between the SERRS and the corresponding RR spectra has been generally attributed to the chemical effects in SERS, but how the proteins change their conformations in the SERS process is still unclear. Furthermore, there is still an ongoing debate on whether the spectrum changes are due to the denaturation of the adsorbed species or due to the selective enhancement of certain vibrational modes.<sup>11</sup> There have been reports claiming that SERS, in essence, measures the photo-products of the analytes.<sup>12</sup> Therefore, SERS is mainly used as a sensitive detection method for quantitative analysis rather than structure characterization. The detail mechanism of the chemical interaction still remains to be fully understood, and an effective

- (1) Fleischmann, M.; Hendra, P. J.; McQuillan, A. *J. Chem. Phys. Lett.* **1974**, *26*, 163–166.
- (2) Jeanmaire, D. J.; Van Duyne, R. P. *J. Electroanal. Chem.* **1977**, *84*, 1–20.
- (3) Albrecht, M. G.; Creighton, J. A. *J. Am. Chem. Soc.* **1977**, *99*, 5215–5217.

- (4) Doering, W. E.; Nie, S. *J. Phys. Chem. B* **2002**, *106*, 311–317.
- (5) Kneipp, K.; Wang, Y.; Kneipp, H.; Perelman, L. T.; Itzkan, I. *Phys. Rev. Lett.* **1997**, *78*, 1667–1670.
- (6) Holman, M. W.; Liu, R.; Adams, D. M. *J. Am. Chem. Soc.* **2003**, *125*, 12649–12654.
- (7) Habuchi, S.; Cotlet, M.; Gronheid, R.; Dirix, G.; Michiels, J.; Vanderleyden, J.; Schryver, F. C. D.; Hofkens, J. *J. Am. Chem. Soc.* **2003**, *125*, 8446–8447.
- (8) Delfino, I.; Bizzarri, A. R.; Cannistraro, S. *Chem. Phys.* **2006**, *326*, 356–362.
- (9) Bjerneld, E. J.; Foldes-Papp, Z.; Kall, M.; Rigler, R. *J. Phys. Chem. B* **2002**, *106*, 1213–1218.
- (10) Bizzarri, A. R.; Cannistraro, S. *Appl. Spectrosc.* **2002**, *56*, 1531–1537.
- (11) Otto, A. *J. Raman Spectrosc.* **2002**, *33*, 593–598.
- (12) Suh, J. S.; Jang, N. H.; Jeong, D. H.; Moskovits, M. *J. Phys. Chem.* **1996**, *100*, 805–813.

way to prevent protein damage from chemical effects has always been in need.

SERS is generally considered to be a result of two main effects: an electromagnetic (EM) effect and a chemical effect. The main contribution arises from the EM effect, a huge enhancement of the local electromagnetic field close to the roughened surface due to the excitation of a localized surface plasmon (LSP). A further enhancement can be observed for molecules adsorbed onto specific sites where the resonant charge transfer occurs.<sup>11,13–15</sup> The chemical effect, which is also referred to as the “first layer” enhancement mechanism, is much smaller than the electromagnetic contribution.<sup>16</sup> The Raman gain due to the EM enhancement ( $G^{(0)}_{\text{SERS}}$ ) is proportional to the fourth power of the ratio of the amplitudes of the local electric fields  $E_{\text{loc}}(\bar{\omega}_{\text{exc}})$  to that of incident electric fields  $E_0(\bar{\omega}_{\text{exc}})$  at the laser angular frequency  $\bar{\omega}_{\text{exc}}$ .<sup>12</sup> This relationship implies that the laser excitation must be located within the resonance plasmon band to obtain high enhancement. It is generally believed that the EM mechanism is based upon the optical properties of the noble metals Ag, Au, and Cu and their ability to support plasmon resonance at visible wavelengths. Therefore, silver and gold nanoparticles are most frequently used as SERS substrates. The resonant excitation of surface plasmons creates an enhanced surface field at both the incoming and outgoing frequencies, resulting in an enhancement of the Raman signal. In the study of biological species, SERS is often coupled with resonance Raman by using a laser excitation wavelength in resonance with the molecular electronic levels (SERRS).<sup>17–24</sup> SERRS not only provides an elevated enhancement but also selectively probes the active site structure of proteins and eliminates the background signal from the protein backbone. For instance, SERRS of heme proteins, using the resonance excitation as in RR, arises mainly from the porphyrin skeletal mode vibrations and peripheral substituents as well as the axial ligand. This can be used to determine the ligation and spin state of the heme, the linkage of the heme group to the proximal ligand, and the interaction with exogenous ligands.<sup>17,25–29</sup> The SERRS spectra of met-myoglobin (metMb) adsorbed on silver colloidal nanoparticles have been obtained in solution at a

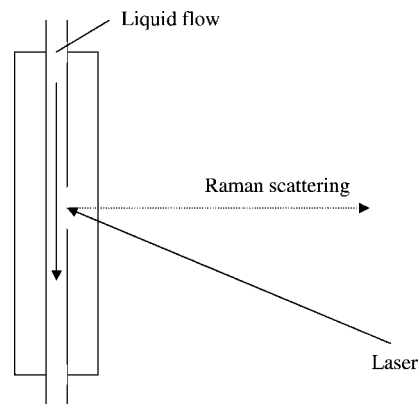


**Figure 1.** Schematic diagram of the flow cell. A solution containing both protein and silver nanoparticles flows through the inner tubing and Raman signal was collected from the open window.

concentration of  $10^{-11}$  M.<sup>10</sup> By controlling the number of nanoparticles in the scattering volume, SERRS for the single molecule detections of heme proteins has also been reported.<sup>10,21–23</sup>

In this work, the SERRS of heme proteins has been studied using a flow system in an effort to understand how proteins change their conformation in the SERRS process and to establish a sensitive method for characterizing the native structure of proteins. A flow system with a home-designed flow cell has been used for this purpose. The results indicate that unlike the conventional SERRS spectra of heme proteins, which are different from their RR spectra, the SERRS spectrum of metMb obtained using the flow system is identical to the resonance Raman spectrum of metMb. Further studies reveal that the strong adsorption of the protein molecules on the surface of nanoparticles disturbs the protein structure and makes it easier to undergo a photoinduced transformation. The laser induced structural transformation process is studied by varying the flow rate and the adsorption time. A comparison of these SERRS spectra, with a focus on the heme oxidation and spin state marker bands, has revealed that the strong adsorption and the exposure to laser irradiation disrupt the distal pocket of the heme group leading to the loss of the distal water. This explains the notion that the SEERS spectrum of metMb obtained using a normal Raman cell is arisen from a 5-coordinated high-spin heme. This observation is important for the correct interpretation of SERRS spectra as well as for understanding the chemical effects in the SERRS process. It also provides clues on how to avoid the protein transformation in SERRS. The new flow system used in this work has proven to be effective in preserving the native structure of the myoglobin molecules. It also offers a potential way to study the native structure of other low concentration level proteins using the SERRS method.

## Experimental Section

**Chemicals.** Horse heart metMb, silver nitrate, and sodium citrate were all obtained from Sigma-Aldrich and were used as received.

**Flow System.** The flow system consists of a peristaltic pump, a T-piece where silver nanoparticles and the protein solution mix, and a Raman flow cell. The peristaltic pump is connected to a computer through an LS-3500 board and is controlled by a computer using an in-house developed program. The key to this system is the flow cell that is made of two concentric tubing (Figure 1). The inner tubing has an open window on which the laser is focused. This design can avoid the deposition of silver granules (aggregates) on the inner cell wall of the normal capillary cells.

- (13) Felidj, N.; Aubard, J.; Levia, G.; Krenn, J. R.; Hohenau, A.; Schider, G.; Leitner, A.; Aussenegg, F. R. *Appl. Phys. Lett.* **2003**, *82*, 3095–3097.
- (14) Otto, A. *J. Raman Spectrosc.* **1991**, *22*, 743–752.
- (15) Aussenegg, F. R.; Lippitsch, M. E. *Chem. Phys. Lett.* **1978**, *59*, 214–216.
- (16) Campion, A.; Kambhampati, P. *Chem. Soc. Rev.* **1988**, *27*, 241–250.
- (17) Feng, M.; Tachikawa, H.; Wang, X.; Pfister, T. D.; Gengenbach, A. J.; Lu, Y. *J. Biol. Inorg. Chem.* **2003**, *8*, 699–706.
- (18) Kneipp, K.; Wang, Y.; Dasari, R. R.; Feld, M. S. *Appl. Spectrosc.* **1995**, *49*, 780–784.
- (19) Kneipp, K.; Wang, Y.; Kneipp, H.; Itzkan, I.; Dasari, R. R.; Feld, M. S. *Phys. Rev. Lett.* **1996**, *76*, 2444–2447.
- (20) Kneipp, K.; Kneipp, H.; Itzkan, I.; Dasari, R. R.; Feld, M. S. *Chem. Rev.* **1999**, *99*, 2957–2975.
- (21) Meixner, A. J.; Vosgrone, T.; Sackrow, M. *J. Lumin.* **2001**, *94–95*, 147–152.
- (22) Michaels, A. M.; Nirmal, M.; Brus, L. E. *J. Am. Chem. Soc.* **1999**, *121*, 9932–9939.
- (23) Michaels, A. M.; Jiang, J.; Brus, L. *J. Phys. Chem. B* **2000**, *104*, 11965–11971.
- (24) Smulevich, G.; Spiro, T. G. *J. Phys. Chem.* **1985**, *89*, 5168–5173.
- (25) Spiro, T. G.; Streckas, T. C. *J. Am. Chem. Soc.* **1974**, *96*, 338–345.
- (26) Tomita, T.; Hirota, S.; Ogura, T.; Olson, J. S.; Kitagawa, T. *J. Phys. Chem. B* **1999**, *103*, 7044–7054.
- (27) Callahan, P. M.; Babcock, G. T. *Biochemistry* **1981**, *20*, 952–958.
- (28) Spiro, T. G.; Stong, J. D.; Stein, P. *J. Am. Chem. Soc.* **1979**, *101*, 2648–2655.
- (29) Smulevich, G.; Miller, M. A.; Kraut, J.; Spiro, T. G. *Biochemistry* **1991**, *30*, 9546–9558.

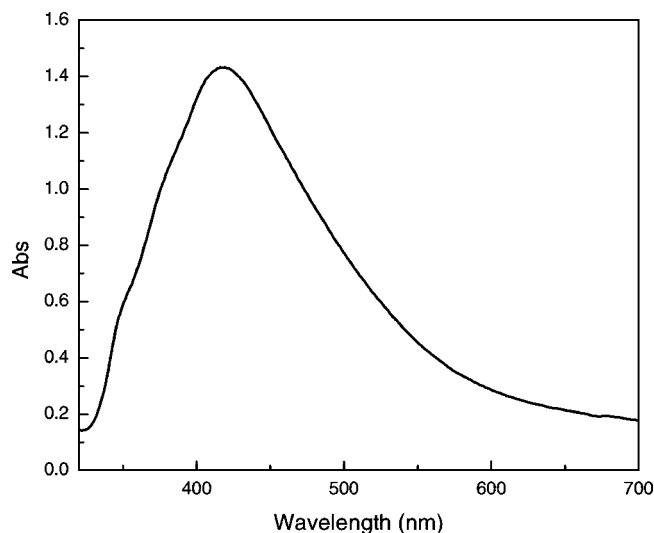


Figure 2. UV-vis absorption spectrum of synthesized silver nanoparticles.

**Preparation of Silver Nanoparticles.** A colloidal silver solution is prepared by the standard citrate reduction of  $\text{AgNO}_3$  by following the procedure of Lee and Meisel<sup>30</sup> with slight modifications. Briefly, in a 125 mL Erlenmeyer flask, 9 mg of silver nitrate (99+ %) was dissolved in 50 mL of deionized water that is preheated to 45 °C. The solution was then brought to boiling, and 10 mL of a sodium citrate solution (1%) was added rapidly with constant stirring. Heating and stirring were maintained for 15 min after adding sodium citrate. The reaction flask was then removed from the heat and allowed to cool to room temperature. The nanoparticles thus prepared show a small effect on the protein structure while maintaining a higher enhancement factor. The nanoparticle suspensions were yellowish brown in appearance.

**Raman Spectroscopy.** Raman spectra were obtained using a Raman spectrometer consisting of a Spex model 1877 triple spectrograph and a CCD detector as reported previously.<sup>17,31</sup> A 406.7-nm line from an argon-krypton ion laser (Spectra-Physics model BeamLokTM 2080-KV) was used as the excitation source, and the Raman signal was collected in a 120° geometry. The laser power was adjusted to ~6 mW at the sample for all measurements. The spectrum collection time for both RR and SERRS was 30 s. Three spectra were coadded to improve the quality of the spectrum. For recording the RR spectrum, 100  $\mu\text{L}$  of a solution containing 0.5 mM metMb in 0.05 M phosphate buffer (pH 6.5) was used. For recording the SERRS spectrum, 5 mL of a solution containing  $1 \times 10^{-7}$  M metMb in 2 mM phosphate buffer (pH 6.5) was used. The frequencies of the Raman bands were calibrated using a standard argon lamp.

A Varian model Cary 300Bio UV-vis spectrophotometer was used to obtain the absorption spectra of nanoparticles as well as those of metMb solutions after mixing with nanoparticle solution. An AMRAY scanning electron microscope and a Digital Instrument model DI3100 atomic force microscope (operated in tapping mode) were used to characterize the synthesized silver nanoparticles.

## Results and Discussions

**Characterization of Silver Nanoparticles.** UV-vis absorption spectroscopy (Figure 2), scanning electron microscopy (SEM), and atomic force microscopy (AFM) were used to characterize the synthesized nanoparticles. The UV-vis absorption spectrum shows a maximum absorption at ~410 nm, demonstrating that the synthesized silver nanoparticles have surface plasmon

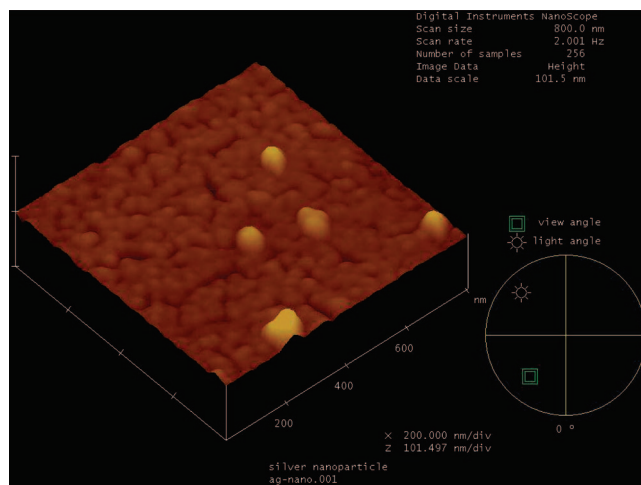


Figure 3. AFM image of silver nanoparticles; the nanoparticles are shown in yellow spheres.

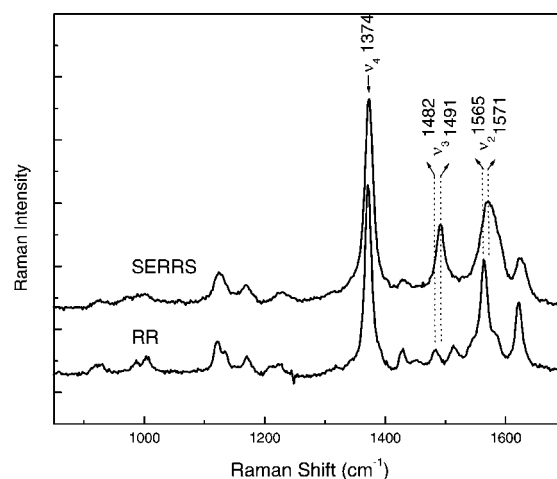


Figure 4. Comparisons of normal SERRS and RR spectra of metMb.

resonance at a wavelength close to the Soret band of heme proteins (409 nm). Therefore, they are ideal for SERRS of heme proteins as the resonance Raman and surface plasmon resonance coincide. Figure 3 is the AFM image of silver nanoparticles indicating that nanoparticles are spherical and have an average particle size of ~70 nm. The size of the nanoparticle is also confirmed by SEM (see Supporting Information).

**Comparison Between the SERRS and RR Spectra of MetMb.** Figure 4 (bottom curve) shows RR spectrum of metMb using a 406.7 nm excitation line. In this frequency range, certain porphyrin Raman modes are marker bands for the heme core-size and iron electronic structure. The  $\nu_4$  mode is sensitive to the iron oxidation state<sup>32</sup> and is found in the frequency range of 1368–1377  $\text{cm}^{-1}$  for ferric hemes and in the range of 1344–1364  $\text{cm}^{-1}$  for ferrous hemes.<sup>25,28,32,33</sup> The Raman mode  $\nu_3$  is sensitive to the heme core-size<sup>33</sup> or to the distance between the pyrrole nitrogen and the heme center (Ct-N).<sup>27,28</sup> The  $\nu_3$  band frequencies are empirically found to be markers of the heme coordination and spin state.<sup>32</sup> For a 6-coordinated high-spin heme, the  $\nu_3$  band normally appears at 1470–1480  $\text{cm}^{-1}$ ,

(32) Abe, M.; Kitagawa, T.; Kyogoku, Y. *J. Chem. Phys.* **1978**, *69*, 4526–4534.

(33) Morikis, D.; Champion, P. M.; Springer, B. A.; Egeberg, K. D.; Sligar, S. G. *J. Biol. Chem.* **1990**, *265*, 12143–12145.

(30) Lee, P. C.; Meisel, D. *J. Phys. Chem.* **1982**, *86*, 391–395.

(31) Feng, M.; Tachikawa, H. *J. Am. Chem. Soc.* **2001**, *123*, 3013–3020.

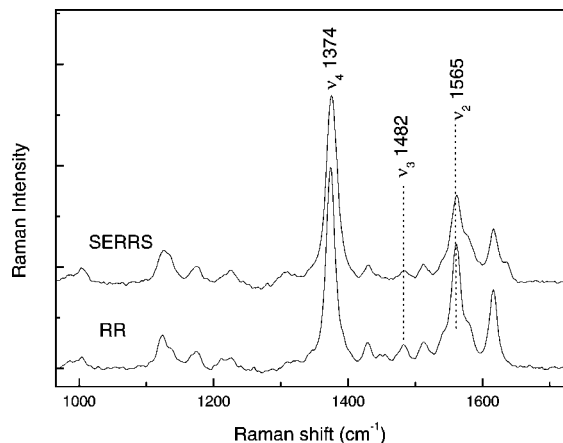


**Figure 5.** SERRS spectrum of metMb using a flow cell and RR spectrum of metMb. Flow rate = 4.6 mL/min, protein concentrations: 0.5 mM for RR and 0.1  $\mu$ M for SERRS,  $\lambda_{\text{ex}}=406.7$  nm, laser power =  $\sim 6$  mW, spectrum collection time =  $3 \times 30$  s.

whereas a 5-coordinated high-spin heme shows a  $\nu_3$  band at 1490–1500  $\text{cm}^{-1}$ , and a 6-coordinated low-spin heme exhibits a  $\nu_3$  band at 1500–1511  $\text{cm}^{-1}$ . Another useful spin marker band is the  $\nu_2$  mode,<sup>32</sup> which appears at  $\sim 1565$   $\text{cm}^{-1}$  for 6-coordinated high-spin heme and at  $\sim 1585$   $\text{cm}^{-1}$  for the 6-coordinated low-spin heme. For high-spin pentacoordinate hemes, this mode appears at  $\sim 1572$   $\text{cm}^{-1}$ . The metMb studied in this paper contains a ferric 6-coordinated high-spin heme. Therefore, the oxidation state marker band  $\nu_4$  is located at 1374  $\text{cm}^{-1}$ . The spin and coordination marker bands,  $\nu_3$  and  $\nu_2$ , are found at 1482 and 1565  $\text{cm}^{-1}$ , respectively, which is in accordance with the expected structure.

In most published results, SERRS spectra were obtained from the proteins adsorbed on a roughened silver electrode or silver nanoparticle colloids. SERRS spectra obtained in this manner are normally different from the RR spectra. Figure 4 (top curve) shows the SERRS spectra of metMb in a silver nanoparticle solution using a spinning Raman cell. Compared with the corresponding RR spectrum of metMb, the SERRS spectrum exhibits several apparent differences. A  $\nu_3$  band that is a marker of both the spin and coordination states appears at 1491  $\text{cm}^{-1}$  in the SERRS spectrum. The  $\nu_2$  band is broadened and shifted to a higher wavenumber at 1571  $\text{cm}^{-1}$ . These results indicate that the SERRS spectrum in this case is from a 5-coordinated high-spin heme. These results suggest that metMb molecules undergo a dramatic conformational change upon interactions with silver nanoparticles and/or laser irradiation. It has been argued that the SERRS spectrum of heme proteins on a roughened silver electrode is from the heme that is detached from the protein despite some reports suggesting that the new features of SERRS spectrum are a result from selected enhancement.<sup>24,34</sup>

**SERRS Spectrum of MetMb Using the Flow Cell.** Figure 5 shows the SERRS spectrum of metMb using the flow cell at a flow rate of 4.6 mL/min (corresponding to a solution moving speed of 2 cm/s). The SERRS spectrum thus obtained (from a  $1 \times 10^{-7}$  M metMb solution) is basically identical to that of the RR spectrum (from a  $5 \times 10^{-4}$  M metMb solution), reflecting the native structure of metMb except for the decrease in the Raman signal compared to the normal SERRS signal using

a conventional cell. The  $\nu_4$  band intensity using the flow cell is about 1/2 of that using a spinning cell under the same condition (using a  $1 \times 10^{-7}$  M metMb solution, a laser power of  $\sim 6$  mW, and collection time of  $3 \times 30$  s). The higher signal intensity using a normal spinning cell is ascribed to the formation of nanoparticle aggregates (see discussion below). This result suggests that the spectral changes observed in the SERRS spectrum using the conventional measurement schemes result from a structural change due to the interaction of protein molecules with the SERRS substrates and the laser irradiation. To gain further understanding of the nature of these interactions, SERRS spectra were recorded using different flow rates. The variation of the flow rate changes the moving speed of the nanoparticles-protein solution and, thus, controls the adsorption time of the protein molecules on the nanoparticles and the exposure time of the adsorbed protein to the laser irradiation. By progressively increasing the flow rate, a series of SERRS spectra were collected. These spectra show a gradual structural change of the protein in a time course during the SERRS experiment. When a high flow rate is used ( $>2.5$  mL/min, which corresponds to a laser exposure time of 0.025 s), the SERRS spectrum is identical to the RR spectrum of metMb as shown. With the decrease of the flow rate from 2 mL/min to 0.1 mL/min (corresponding to a laser exposure time from 0.03 to 0.3 s) the SERRS spectra show a gradual change marked by the disappearance of the  $\nu_{38}$  band<sup>28,35</sup> (1514  $\text{cm}^{-1}$ ) and a broadening and gradual shifting of the  $\nu_3$  band from 1482 to 1491  $\text{cm}^{-1}$ . In addition, the  $\nu_2$  band also broadens and shifts from 1565 to 1572  $\text{cm}^{-1}$ . These results imply the formation of a 5-coordinated high-spin state of metMb. Besides the frequency change of these marker bands, the SERRS intensity is also affected by the flow rate. For example, the intensity of the  $\nu_4$  band slightly decreases with a decrease in the flow rate. The decrease in Raman intensity at a lower flow rate is possibly due to the laser-induced damage to the samples.

In its native form, metMb contains a heme that is in a 6-coordinated high-spin state with water as the distal ligand. The distal water is stabilized through H-bonding with the amino acid residues in the heme pocket (the distal histidine His64). There have been several reports indicating that changes in the heme pocket generally lead to the absence of the distal water molecule. The pentacoordinated ferric hemes have been suggested in globins, which lack a distal histidine or other residues that can hydrogen-bond to a water molecule.<sup>36,37</sup> The replacements of the distal and proximal histidines in Mb mutants have also shown to expel the distal water and favor a pentacoordinated heme iron.<sup>33</sup> Disruption of the hydrogen bonding in addition to the increase of heme pocket hydrophobicity by these mutations have been ascribed to the formation of pentacoordinated hemes.<sup>33</sup> In metMb, the His64 residue is connected to a  $\alpha$ -helix that consists of the sequence from ASP60 to LYS77. Because the  $\alpha$ -helix is on the surface of the protein, its conformation tends to be disturbed when the protein molecules approach the nanoparticle surface. The conformation motion induced by this interaction may drive His64 from its original position and, in turn, disrupt the H-bonding network leading to the escape of the distal water. The laser illumination further promotes this

(35) Parthasarathi, N.; Hansen, C.; Yamaguchi, S.; Spiro, T. G. *J. Am. Chem. Soc.* **1987**, *109*, 3865–3871.

(36) Rousseau, D. L.; Ching, Y. C.; Brunori, M.; Giacometti, G. M. *J. Biol. Chem.* **1989**, *264*, 7878–7881.

(37) Dasgupta, S.; Rousseau, D. L.; Anni, H.; Yonetani, T. *J. Biol. Chem.* **1989**, *264*, 654–662.

(34) Cotton, T. M.; Schultz, S. G.; Van Duyne, R. P. *J. Am. Chem. Soc.* **1980**, *102*, 7960–7962.

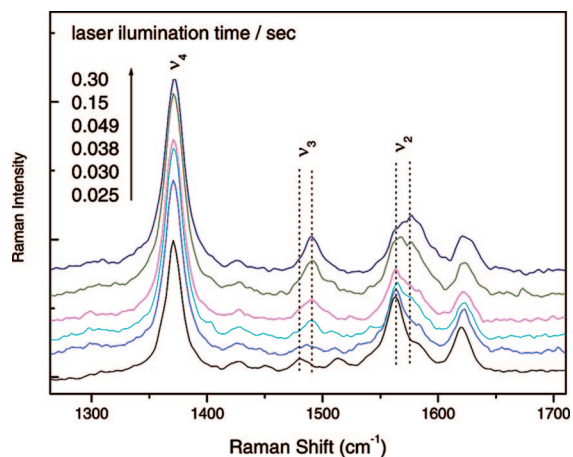


**Figure 6.** SERRS spectra of metMb with different laser-exposure-time durations. Flow rate = 4.6 mL/min, protein concentration = 0.1  $\mu$ M,  $\lambda_{\text{ex}}$  = 406.7 nm, laser power =  $\sim$ 6 mW, spectrum collection time =  $3 \times 30$  s.

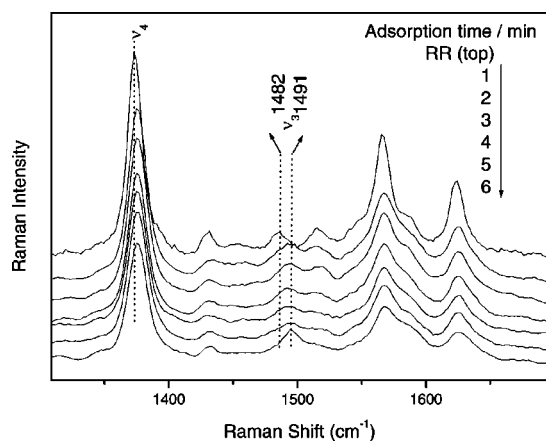


**Figure 7.** SERRS spectra of metMb after incubation with silver nanoparticles for different time durations. Flow rate = 4.6 mL/min, protein concentration = 0.1 M,  $\lambda_{\text{ex}}$  = 406.7 nm, laser power =  $\sim$ 6 mW, spectrum collection time =  $3 \times 30$  s.

interaction and causes the disruption and/or even the collapse of the heme pocket structure (Figure 6). It should be noted that, with a lower flow rate (corresponding to a laser exposure time of greater than 0.3 s), the SERRS spectra exhibit some further changes such as a broadening of the  $\nu_2$  (at 1572  $\text{cm}^{-1}$ ) and  $\nu_{10}$  modes (at 1623  $\text{cm}^{-1}$ ). This may imply a further change of the protein structure (even the detachment of the heme). At a lower flow rate, the  $\nu_4$  band also shifts slightly ( $\sim$ 2  $\text{cm}^{-1}$ ) to higher frequencies. The shift in the  $\nu_4$  mode frequency may be due to a charge-transfer from silver to the heme porphyrin ring implying a closer contact of the protein with the nanoparticles and a stronger interaction between them.

**Effects of Protein–Nanoparticle Interactions.** In most of the reported SERRS experiments, the analytes are normally incubated with the nanoparticle colloids for a certain period of time to allow the adsorption of the analytes and to gain better sensitivity.<sup>9,10,22</sup> Yet, there is a question whether this adsorption process affects the protein structure. To examine the adsorption effects, the metMb solution was incubated with silver nanoparticles for a certain period of time prior to the SERRS measurements. Figure 7 shows SERRS spectra of metMb after incubating the solution for several different periods of time. A flow rate of 4.6 mL/min was used for collecting these spectra. The SERRS spectrum of metMb with a shorter incubation time

shows a spectrum closer to the RR spectrum of metMb. With an increase in the incubation time, the spectrum changes gradually indicating the change of the heme group from a 6-coordinated high-spin state to a 5-coordinated high-spin state. This result suggests that the adsorption of the protein molecules on the nanoparticle surface disturbs and even alters the protein structure. It is possible that the electrostatic interaction between the proteins and the nanoparticles is the main force accounting for the strong interaction. Mb with a  $pI$  of 6.85 (acidic band) to 7.35 (basic band)<sup>38</sup> is positively charged at the experimental pH of 6.5. On the other hand, the silver nanoparticles synthesized by citrate reduction have a negatively charged organic surface layer as indicated by the overall zeta charge of around  $-40$  mV.<sup>39</sup> The electrostatic interaction, which is the initial driving force of the protein adsorption on the nanoparticles, is the prelude of further chemical interactions (such as the charge transfer between the silver and the heme group and the change of the coordination state). Another evidence for the changing of the protein structure is the slight decrease of the SERRS signal with the increase in the adsorption time. The prolonged adsorption makes the protein less stable and more susceptible to the laser-induced decomposition.

The adsorption effect on the protein structure is also confirmed by UV–vis absorption spectroscopy. The metMb in its native form exhibits a strong Soret band at 409 nm and a weak visible band at 504 nm. These absorption bands originate from the prosthetic heme group which is embedded in a hydrophobic pocket formed by the protein's backbone through appropriate folding. Any exogenous factors that affect the protein structure will have impact on the heme pocket structure and will reflect in the UV–vis absorption spectrum. Figure 8 shows the UV–vis absorption spectra of metMb recorded consecutively at one-minute intervals after mixing the metMb solution with the silver nanoparticle solution. These spectra demonstrate a progressive decrease of the Soret band and a red shift of the visible band with increased absorbance. The spectrum reaches a stable state after 10 min. These changes indicate the disturbing of the heme pocket structure and the exposure of the heme group to the aqueous medium. When the stabilized metMb–nanoparticle solution (i.e., the absorption spectrum reaches the stable state after incubation) is exposed to laser irradiation, a further decrease of the Soret band is noticed. These results indicate that the laser irradiation further disrupts the protein structure. It is interesting to note that the absorption band of metMb at 280 nm remains unchanged after the incubation process indicating that the protein molecules maintain a native secondary structure.

**Effects of the Nanoparticle Aggregation.** It has been reported that the aggregation of nanoparticles creates a microstructure with high surface plasmon resonance and greatly enhances the SERRS signals. During this study using a conventional Raman cell, we have noticed that laser irradiation induces the formation of nanoparticle aggregates when protein molecules are adsorbed on the nanoparticle surface. This is evidenced by the color change (from yellowish to dark brownish) of the protein–nanoparticle mixture upon exposure to the laser. Other evidence is that granules are always found on the inner surface of the capillary when a capillary flow cell is used. SERRS spectra of metMb from the silver aggregates (formed by using normal

(38) Cotoras, M.; Silva, E. *Mycologia* **2005**, *97*, 485–492.

(39) Graham, D.; Faulds, K.; Smith, W. E. *Chem. Commun.* **2006**, 4363–4371.

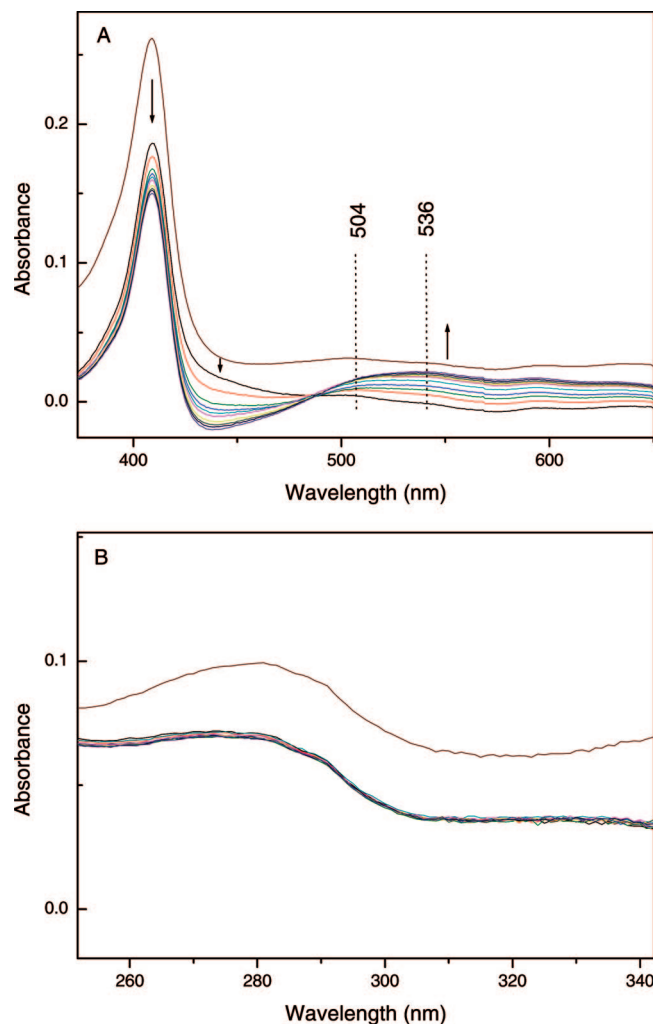


**Figure 8.** UV-vis absorption spectra of metMb solution (1  $\mu\text{M}$ ) during the incubation with silver nanoparticles: (A) changes of the Soret and visible bands of metMb and (B) changes of the UV absorption band of metMb. The spectra were recorded at one-minute intervals. An absorption spectrum of metMb (offset for better viewing) in a pH 6.5 phosphate buffer is added (top) for reference in each spectrum range.

spinning Raman cell) show a signal about 2 to 3 times higher than that of the SERRS spectra using the flow cell (in reference to the intensity of the  $\nu_4$  band). However, the spectra obtained by using the spinning Raman cell always show the features of a 5-coordinated high-spin heme. This observation indicates that (1) the nanoparticle aggregates have a strong interaction with the protein molecules leading to the chemical effects and changes of the protein structure and (2) the aggregates produce a microstructure that provides higher enhancement factors. The SERRS spectra of Mb from aggregated silver nanoparticles also show a slight shift of the  $\nu_4$  band, confirming the formation of

a surface metal-protein (M-P) complex and the charge-transfer effects<sup>40</sup> originating from the photoinduced charge donation from the metal surface to the adsorbate or vice versa. It has been reported that the SERS enhancement from chemical effects could be ascribed to the charge transfer between the neighboring metal nanoparticles tunneling through the interconnected analyte molecules.<sup>41</sup> The enhancement from the CT mechanism was previously observed from the interconnecting 4-aminothiophenol (PATP) molecules between the particles<sup>41</sup> that are dependent on the assembly form of the metal particles and the direction of the molecular dipole. The nanoparticle aggregation creates a microstructure with curvatures and tunnels that favors the formation of metal-protein-metal junctions and leads to the charge-transfer effects.

## Conclusions

It is still a big challenge to obtain experimental evidence that are independently associated with the EM or CT mechanism in SERS because the two effects are normally inextricably linked. With an in-house designed flow cell, a SERRS spectrum of metMb that is free from chemical effects has been observed at a higher flow rate because the observed SERRS spectrum is basically the same as the corresponding RR spectrum. However, the chemical mechanism starts to take effect when a slower flow rate is used or proteins are allowed to adsorb on the metal surface. The initial evidence of this interaction in the case of metMb is a shift of the oxidation state marker band. The additional interaction of proteins with the SERRS substrate and laser irradiation further changes the protein structure. The Raman flow cell system described in this work is not only a useful tool to gain in-depth experimental insight into the SERRS mechanism but also eliminates the photoinduced structural changes of proteins in normal SERRS experiments by providing an effective way to sensitively characterize the native structure of biological materials.

**Acknowledgment.** This work was supported in part by the National Institutes of Health (Grant S06GM008047 and NIH-RCMI G12RR13459). The authors thank Dr. Kenneth R. St. John (The University of Mississippi Medical Center) for obtaining SEM image of silver nanoparticles.

**Supporting Information Available:** SEM image of silver nanoparticles. This material is available free of charge via the Internet at <http://pubs.acs.org>.

JA8006337

(40) Arenas, J. F.; Fernandez, D. J.; Soto, J.; Lopez-Tocon, I.; Otero, J. C. *J. Phys. Chem. B* **2003**, *107*, 13143–13149.

(41) Zhou, Q.; Zhao, G.; Chao, Y.; Li, Y.; Wu, Y.; Zheng, J. *J. Phys. Chem. C* **2007**, *111*, 1951–1954.